

Neutral Gas Accretion onto Nearby Galaxies

Felix J. Lockman

Abstract While there is no lack of evidence for the accretion of stellar systems onto nearby galaxies, direct evidence for the accretion of gas without stars is scarce. Here we consider an inventory of starless gas “clouds” in and around galaxies of the Local Group to discern their general properties and see how they might appear in distant systems. The conclusion is that accreting gas without stars is detected almost entirely within the circumgalactic medium of large galaxies and is rare otherwise. If our Local Group is any example, the best place to detect starless gas clouds is relatively close to galaxies.

1 Galaxies Then and Now

The evidence at present available points strongly to the conclusion that the spirals are individual galaxies, or island universes, comparable with our own galaxy in dimensions and in number of component units. – H.D. Curtis

... the extraplanar gas seems to consist of two parts: a large one from galactic fountains and a smaller part accreted from intergalactic space. There is direct (HVCs in our galaxy and filaments in external galaxies) and indirect (rotational velocity gradients) evidence for the accretion from outside. — Sancisi et al. 2008

Galaxies are like people. Every time you get to know one well, it turns out to be a little peculiar. – Sidney van den Bergh

Unlike the days of the *Island Universe*, when galaxies floated in solitary splendor on Hubble’s Tuning Fork (Hubble, 1958), today’s galaxies are a mess (Fig. 1). Evidence for the growth and evolution of galaxies by the capture of stellar systems is

Felix J. Lockman

Green Bank Observatory, e-mail: jlockman@nrao.edu. The Green Bank Observatory is a facility of the National Science Foundation, operated under a cooperative agreement by Associated Universities, Inc.

everywhere and there are arguments for continued accretion of gas as well. Certainly some gas will arrive with the small stellar systems that large galaxies devour, but how does it get to the disk, and is there neutral gas accreting from other sources? In this article I consider the evidence for accretion of neutral gas onto nearby galaxies, especially gas that is not associated with stars. This is not a comprehensive review, but instead explores the connection between gas likely to be accreting onto galaxies in the Local Group, where we can examine it with high sensitivity and linear resolution, and that seen in more distant systems with a better vantage but considerably less sensitivity. Is there local accretion of starless gas, and what form does it take?

Two comprehensive reviews are directly relevant to this topic. Sancisi et al. (2008) consider the evidence for accretion of neutral gas by analyzing high resolution HI maps of several dozen nearby galaxies. They find ample evidence of kinematic anomalies, tails and filaments, warps, lopsided disks, and interaction. They adopt the stance that any significant deviation of a galaxy's HI from symmetry is evidence for interaction, and that interaction implies accretion. Accretion also has a prominent place in the recent review of gaseous galaxy halos by Putman et al. (2012) which takes a thorough look at circumgalactic gas in all phases. I will refer to these reviews throughout this article for more complete discussion of some topics.



Fig. 1 Examples of stellar accretion in two galaxies from Carlin et al. (2016). Images on the left from the Sloan Digital Sky Survey of the nearby galaxies NGC 4013 (top) and M 63 (bottom) show regular disks while the much deeper images on the right reveal streams of stars accreted from smaller galaxies.

The volume around galactic disks contains material in many forms. Both the Milky Way (MW) and M31 have a hot 10^{6-7} K circumgalactic medium (CGM) of enormous mass and extent, possibly dwarfing the baryon content of the disks themselves (Anderson & Bregman, 2011; Hodges-Kluck et al., 2016; Lehner et al., 2015). This gas may cool and condense, feeding the disk. There may also be cosmological accretion – cold flows – which may have to traverse the CGM to reach the disk and in that passage may be disrupted entirely (Putman et al., 2012). Then there is gas that has been stripped from one galaxy through interaction and ultimately ends up in the disk of another. Add to that the ejection of gas from a galaxy’s disk from supernovae or a nuclear wind, and the processes can become quite difficult to disentangle. Considerable insight into the the CGM of galaxies has come through studies of Ly α and MgII absorption lines (Kacprzak et al., 2013; Wakker & Savage, 2009), but those data will not be discussed here. Instead, we will concentrate on 21cm HI observations, and work from the inside out, from the interstellar medium (ISM) disk-halo interface, to high velocity clouds (HVCs), to the products of interaction between galaxies, and finally to HI ”clouds” that don’t easily fit into any of these categories.

But first a note on the detectability of HI. Filled-aperture (single dish) radio telescopes can easily detect HI column densities of $N_{\text{HI}} = 10^{18} \text{ cm}^{-2}$, and with a little work, 10^{17} cm^{-2} . This comes at the expense of angular resolution, which for modern instruments is in the range $3' - 10'$. Hydrogen clouds with $M_{\text{HI}} \geq 10^5 M_{\odot}$ can thus be detected anywhere in the Local Group at a linear resolution of 1–3 pc d_{kpc} . Aperture synthesis instruments provide much higher angular resolution of $< 1'$ but at the cost of reduced sensitivity. The smallest object in the table of plumes, wings, and other peculiar HI structures of Sancisi et al. (2008) has $10^8 M_{\odot}$. The deepest aperture synthesis HI observations of galaxies so far have come from the HALOGAS survey Heald et al. (2011) which reaches a limiting sensitivity of $N_{\text{HI}} = 10^{18.5-19.0} \text{ cm}^{-2}$.

This sensitivity gap is not unbridgeable, but we should keep it in mind when comparing local with distant objects.

2 The Disk-Halo Interface: Clouds and Shells

The Milky Way gives us a close view of process like the galactic fountain, which lifts gas several kpc away from a spiral galaxy’s disk (Shapiro & Field, 1976; Bregman, 1980). Figure 2 shows Milky Way HI along a cut $\sim 20^\circ$ in longitude through the Galactic plane approximately along the tangent points. It is easy to find HI loops, filaments, clouds and a diffuse component extending many degrees away from the plane. In this figure each degree of latitude corresponds to a displacement ≈ 135 pc from the midplane, so the HI emission at $b = \pm 4^\circ$ arises in neutral gas at a height $z \sim 0.5$ kpc, several HI scale heights above the main HI layer (Dickey & Lockman, 1990). In the inner Milky Way about 10% of the HI can be found more than 0.5 kpc from the disk (Lockman, 1984). Some of this HI is contained in discrete clouds

that can be identified to $z \approx 2$ kpc (Lockman, 2002; Ford et al., 2010). Some of the extraplanar HI is also organized as large "supershells", whose tops can reach $|z| > 3$ kpc. They can be ~ 1 kpc in size and contain $3 \times 10^4 M_{\odot}$ of neutral gas (Heiles, 1979; McClure-Griffiths et al., 2002; Pidopryhora et al., 2007).

Supershells certainly have their origin in supernovae and stellar winds (Tomisaka & Ikeuchi, 1986), and can often be linked directly to sites of star formation (Pidopryhora et al., 2007; Kaltcheva et al., 2014). The cloud-like component of extraplanar HI has a less certain origin, though it may result from the breakup of shells. Often referred to as "disk-halo" clouds, they appear to be related both spatially and kinematically to the disk, though the population extends well into the lower halo (Lockman, 2002; Ford et al., 2010). Some of the larger Milky Way disk-halo clouds with $M_{\text{HI}} \approx 500 M_{\odot}$ have been imaged at 2-3 pc resolution and show a variety of shapes with some sharp boundaries and evidence of a two-component thermodynamic structure (Pidopryhora et al., 2015). Note that from the above discussion on sensitivity, these disk-halo clouds could not be detected beyond the Milky Way as individual objects. Within the Milky Way there is a general correlation between the amount and vertical extent of disk-halo clouds and the spiral arms (Ford et al., 2010) although there is no detailed correlation with individual star-forming regions.

A similar extraplanar HI layer is seen in a number of galaxies, often containing 10% of the disk HI mass, though the percentage has large variations from galaxy to galaxy (Sancisi et al., 2008). While it is not possible to isolate individual disk-halo

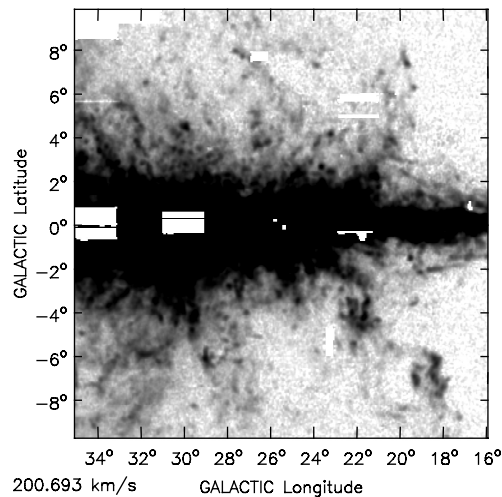


Fig. 2 Cut through the Galactic plane at velocities approximately along the tangent point showing the vertical extent of Galactic HI. In this projection a latitude of 8° corresponds to a distance ~ 1 kpc from the Galactic plane. These observations can resolve structures down to a few 10s of pc in size.

clouds in other galaxies, the better vantage afforded in observations of extragalactic systems allows the kinematics of this component to be analyzed more completely. The disk-halo (or extraplanar) gas often shows evidence of a vertical lag in rotational velocity of $10 - 20 \text{ km s}^{-1} \text{ kpc}^{-1}$ but with a large range; sometimes an inflow toward the center of a galaxy is also inferred at the level of $10\text{-}20 \text{ km s}^{-1}$ (Fraternali et al., 2002; Sancisi et al., 2008; Zschaechner et al., 2015). This extraplanar gas does not show large deviations from prograde galactic rotation, and constitutes a dynamic neutral galactic atmosphere.

The disk-halo gas extends to heights where it may mix with material accreting through or cooling from the CGM (Putman et al., 2012). Thus the presence of neutral gas many scale-heights away from the plane is not unexpected, and distinguishing between gas that is "recycled" as much of the disk-halo material must be, and gas that has never been in the disk, may not be straightforward in the absence of other information. Although the disk-halo clouds are concentrated to the disk in the sense that their numbers increase towards the disk, there is no way to know if any individual cloud had its origin in the Milky Way, or has been accreted, or is a combination of both processes (Marasco et al., 2012). It would be very interesting to have information on the elemental abundances in disk-halo clouds at different heights.

Any gas accreting onto the Milky Way has to pass through the extended disk-halo layer before it reaches the inner disk. One massive cloud passing through this layer shows evidence of disruption, and is discussed in section 3.2.

3 High Velocity Clouds

It has been known for more than 50 years that there are significant amounts of neutral hydrogen around the Milky Way that do not follow Galactic rotation – the high velocity clouds (HVCs) (Muller et al., 1963; Wakker et al., 2004). For many years the lack of information on their distances has allowed speculation that some of them might be $\sim 1 \text{ Mpc}$ or more away from the Milky Way and thus have $M_{\text{HI}} = 10^{7-8} M_{\odot}$ (Blitz et al., 1999; Braun & Burton, 1999). However, the discovery of a similar population around M31, M33, and other galaxies (Thilker et al., 2004; Westmeier et al., 2008; Grossi et al., 2008; Putman et al., 2009; Keenan et al., 2016; Miller et al., 2009), suggests that the phenomenon is likely common and, as importantly, confined to the inner CGM of spirals. This does not mean that some of the more compact, more isolated HVCs might not be free-floating independent systems, but the total HI mass within the CGM of normal galaxies (aside from the products of tidal interaction) must be relatively small (Pisano et al., 2007, 2011). The HVC system of the Milky Way has been estimated to contain an HI mass of $\sim 3 \times 10^7 M_{\odot}$ (Putman et al., 2012). The HVC population likely contains as much ionized gas as neutral gas (Shull et al., 2009, 2011; Lehner & Howk, 2011).

One of the most important facts about HVCs is that they do not contain stars (Hopp et al., 2007). In this sense, compact HVCs that are discovered to be dwarf

galaxies (e.g. Leo P; Rhode et al., 2013), are simply objects that have been misclassified as HVCs. Another important property is that their velocities are not really that high: none have velocities near or greater than the escape velocity of the Milky Way (Wakker et al., 2004). Putman et al. (2012) estimate that the larger Milky Way HVCs have kinematics that can be fit by a prograde rotational component about one-third the circular velocity of the Sun, and an inflow component of a few tens of km s^{-1} , though one prominent cloud almost certainly has a large retrograde motion (Lockman, 2003).

3.1 High Velocity Clouds in M31 and M33

The HVC population of M31 is shown in Figure 3. The typical M31 HVC has M_{HI} of a few $10^5 M_{\odot}$, and would not be detectable as an individual object in most measurements of more distant galaxies. The right panel of Fig. 3 emphasizes the proximity of HVCs to that galaxy's disk, and the difficulty one would have in disentangling them from the disk-halo layer in more distant systems. The HVCs of M31 seem to be confined to within 50 kpc of that galaxy, though there are indications that some may be found to greater distances to the north (Westmeier et al., 2008; Wolfe et al., 2016). The total HI mass in the M31 HVCs is $2 \times 10^7 M_{\odot}$; when extraplanar gas possibly associated with the disk is included, the amount may be as high as $5 \times 10^7 M_{\odot}$ (Westmeier et al., 2008).

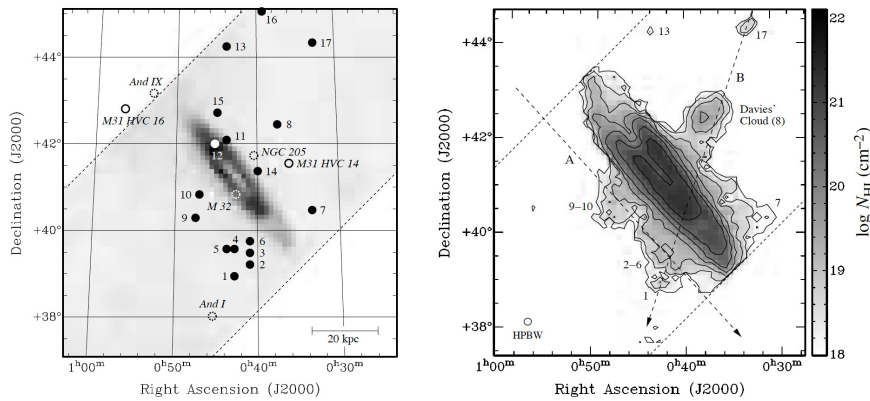


Fig. 3 From Westmeier et al. (2008). Left panel: the HVC system of M31 in relationship to the bright HI in the disk. Right panel: integrated HI over all velocities with contours at $\log_{10}(N_{\text{HI}})$ 18, 18.5, 19, 19.5, Many of the HVCs seem to blend into the disk, but in maps at different velocities it is clear that they are distinct objects. This is how M31 would appear to current instruments were it ~ 10 Mpc distant, except that the two lowest contours would be missing. As noted by Putman et al. (2012) this image of M31 bears a strong resemblance to the HI image of the galaxy NGC 891 (Oosterloo et al., 2007) which has been observed with about the similar linear resolution as M31.

There are also HVCs around M33, though here confusion with that galaxy's disk and possibly unrelated extraplanar gas makes it difficult to separate the populations cleanly (Grossi et al., 2008; Putman et al., 2009; Keenan et al., 2016). The total HI mass in the M33 HVCs is $3.5 \times 10^7 M_{\odot}$ using only the data from the most recent study (Keenan et al., 2016). If we include clouds that may be located in the disk-halo region (Grossi et al., 2008; Putman et al., 2009) the total M33 HVC HI mass increases to $\sim 5 \times 10^7 M_{\odot}$.

Figure 4 shows the velocity and location of the HVCs of M31 and M33 with respect to M31. At the distance of these galaxies one degree on the sky corresponds to about 15 kpc. This figure includes some objects in M33 (marked in blue) that are probably part of the disk-halo interface and not true HVCs (Putman et al., 2009; Keenan et al., 2016), but are included to show that aspects of these two populations can blend and they often occupy very similar areas of position and velocity space. This figure shows another interesting aspect of HVCs. The velocity spread of those associated with M33 is considerably smaller than those associated with M31. If HVCs are condensations from the CGM this would follow naturally, as M33 is less massive than M31 and so presumably has a CGM that rotates more slowly.

A key fact that has been established through distance measurements to Milky Way HVCs and studies of M31 and M33 is that HVCs are not free-floating in the Local Group, but are concentrated around the large spirals. If the HVCs are even in approximate pressure equilibrium with a galaxy's CGM they must be orders of magnitude more dense than the hot gas around them and thus falling toward the disk. There is some evidence for the interaction of Galactic HVCs with the CGM in the form of distortions of the cloud shapes (Brüns et al., 2000), and there is rather spectacular evidence for the direct accretion of HI onto the Milky Way from one HVC: The Smith Cloud.

3.2 The Smith Cloud – Accretion in Action

In the same year that the discovery of HVCs was announced, a short paper appeared reporting observations of a peculiar HI feature that now appears to be a very important object, the Smith Cloud (Smith, 1963). Figure 5 shows an HI channel map from a recent 21cm survey made with the Green Bank Telescope (GBT). The cloud has a good distance estimate (Wakker et al., 2008), and thus a well defined mass and size; it is moving toward the Galactic plane, which it should intersect in ~ 30 Myr if it survives as a coherent entity (Lockman et al., 2008). Its mass in HI is $\sim 2 \times 10^6 M_{\odot}$ and it has an ionized component with a similar mass detected in faint H_{α} emission (Hill et al., 2009). There is evidence that it has a magnetic field $\approx 8\mu\text{G}$ (Hill et al., 2013) and a S/H abundance that is about one-half Solar (Fox et al., 2016). Its total space velocity is below the escape velocity of the Milky Way, and the largest component is in the direction of Galactic rotation. It appears to be entering the Milky Way at a rather shallow angle (Lockman et al., 2008; Nichols &

Bland-Hawthorn, 2009). The Smith Cloud is thus adding angular momentum to the disk. It has no detectable stars (Stark et al., 2015).

The brightest, most compact component of the Cloud lies about 3 kpc below the Galactic plane. It is thus in the disk-halo transition, and it appears that it is encountering a clumpy medium. The Cloud has holes that are matched by small fragments at 60 km s^{-1} lower velocity, consistent with the velocity of the Milky Way's halo at that location (Fig. 6). This object shows clear signs of interaction with the Milky Way's extraplanar gas.

There are many puzzles surrounding the Smith Cloud. If it has condensed from the CGM than why does it have a S/H metallicity ratio higher than typical HVCs (Fox et al., 2016; Wakker et al., 2004)? If it originated from the Galaxy, then how did it acquire such a large peculiar motion and mass, which implies a kinetic energy $\sim 5 \times 10^{53}$ ergs (Marasco & Fraternali, 2017)? Does it require a significant dark matter component to maintain its stability, as suggested by some investigations (Nichols & Bland-Hawthorn, 2009; Nichols et al., 2014)?

If the Smith Cloud were at the distance of M31 it would appear to the HVC surveys with a peak N_{HI} around $2 \times 10^{19} \text{ cm}^{-2}$, a few times higher than the M31 HVCs, but not especially anomalous. With an M_{HI} of $2 \times 10^6 M_{\odot}$, the Smith Cloud has about the median HI mass of the M33 HVCs and lies at the upper range of those around M31. Given the observational uncertainties, the Smith Cloud would be an inconspicuous addition to either galaxy (Lockman et al., 2008; Westmeier et al., 2008; Keenan et al., 2016). However, as the brighter parts of the Smith Cloud lie only ~ 3 kpc away from the Galactic plane, if it were at the distance of M31 or M33 it would lie projected on the disk of those galaxies, and from even the most favorable vantage would be separated by only $12'$ from their disk. It would almost certainly be considered part of the disk-halo interface and not cataloged as an HVC.

Some HVCs in M31 and M33 have linewidths $> 50 \text{ km s}^{-1}$, suggesting large internal motions or disruption (Westmeier et al., 2008; Keenan et al., 2016). If the Smith Cloud were at the distance of M31, our poorer linear resolution would blend its different components, raising its HI linewidth from the $< 20 \text{ km s}^{-1}$ that we typically measure in its brighter parts, to 40 km s^{-1} .

4 HI Outside Local Group Galaxies

The Local Group contains two wonderful examples of HI without stars, both associated with the Magellanic Clouds: the Magellanic Stream (MS) and the Leading Arm (LA). These are the rather enormous streams of gas (containing about 10% the mass of the Milky Way's ISM) that are currently being lost from the Magellanic Clouds and are entering the Milky Way's CGM. A distance of 55 kpc is assumed for both objects, though this has a large uncertainty; for a recent review see D'Onghia & Fox (2016). The relevant HI masses are $3 \times 10^8 M_{\odot}$, and $3 \times 10^7 M_{\odot}$, for the Stream and Leading Arm, respectively (Brüns et al., 2005). The total mass of the Stream is $\sim 10^9 M_{\odot}$, and is dominated by ionized gas (Fox et al., 2014). The Magellanic

Clouds are the only stellar systems in the Local Group that are observed to be losing their gas. The Magellanic Stream is important for our purposes because it gives us a model for how we might interpret observations of other systems. Although the combined MS + LA is 200° long (Putman et al., 2003; Nidever et al., 2010) I estimate that no more than half this length would appear with $N_{\text{HI}} > 10^{19} \text{ cm}^{-2}$ at a few Mpc distance, and thus be detectable in 21cm HI emission in another galaxy group. The detectable part of the MS would have a length ~ 100 kpc and for the Leading Arm, about 60 kpc.

Although we can see that the Stream and the Leading Arm are anchored in the stellar systems of the Magellanic Clouds, there are no stars associated with the gas of either object (D’Onghia & Fox, 2016). The absence of stars in the gas mirrors the fact that none of the stellar streams around the Milky Way or M31 have been found to have a convincing association with any neutral gas (Lewis et al., 2013).

The Milky Way’s CGM seems quite resistant to the passage of neutral gas clouds even when they are attached to galaxies. Dwarf spheroidals within a few 100 kpc of the Milky Way seem utterly devoid of HI: the limits on some systems with $L_* \approx 2.5 \times 10^5 L_\odot$ are smaller than $100 M_\odot$ (Spekkens et al., 2014). A similar deficit is found for the dwarf satellites of M31 (Beaton, private communication). Because dwarf galaxies > 400 kpc from the Milky Way seem to have retained their gas, the deficit for nearer dwarfs presumably reflects their stripping by the CGM (Blitz & Robishaw, 2000; Grcevich & Putman, 2009). Distant dwarfs have $M_{\text{HI}}/L_* \approx 1$ (Spekkens et al., 2014), so we can estimate the HI mass that has been deposited in the CGM through this stripping. For the dwarf galaxies currently known around the Milky Way, it amounts to $M_{\text{HI}} \approx 3 \times 10^7 M_\odot$, an value almost identical to the estimated total HI mass of HVCs in each of the HVC systems of the Milky Way, M31, and M33 (Putman et al., 2012; Westmeier et al., 2008; Keenan et al., 2016). It is tempting to dismiss this as a coincidence, especially because the inferred mass of the “stripped” HI for the Milky Way is dominated by the most massive galaxy, the Sagittarius dSph (Spekkens et al., 2014). But we do not have a good understanding of the inflow rate and location of the stripped material, which likely eventually make its way to the disk.

5 Other Neutral Gas in the Local Group

5.1 IC 10

This blue compact dwarf galaxy, a satellite of M31, is undergoing a burst of star formation and has a complex HI structure with counter-rotating components and two tails or streamers shown in Figure 7 (Shostak & Skillman, 1989; Nidever et al., 2013; Ashley et al., 2014). Kinematic analysis of the HI suggests that the gas is inflowing rather than outflowing. Its stellar component, however, does not show evidence of streams or shells, or any kind of disturbance, though the young stellar

populations are spatially offset from the older stellar population (Gerbrandt et al., 2015). The data thus suggest that IC 10 is accreting nearly starless gas and not a companion. The mass in the southern and northern HI features is $10^7 M_{\odot}$ and $6 \times 10^5 M_{\odot}$, respectively, out of a total M_{HI} for the entire system of $8 \times 10^7 M_{\odot}$. The disturbed material is a significant fraction of the gas mass. It is interesting that the two anomalous HI features of IC 10 lie approximately on a line pointing back toward M31.

With a stellar mass of $8.6 \times 10^7 M_{\odot}$ (McConnachie, 2012), IC 10 has a $M_{\text{HI}}/L_V \approx 1$, similar to gas-rich Local Group dwarfs, even though it is only 250 kpc from M31 and thus is not only a satellite of M31, but lies well within the CGM of that galaxy. IC 10 and the Magellanic Clouds appear to be the only gas-rich dwarf galaxies within a few hundred kpc of the Milky Way or M31 in the Local Group, and the Magellanic Clouds are losing their gas while IC 10 seems to be accreting.

5.2 M31-M33 Clouds

In a map that reached a sensitivity to N_{HI} of a few 10^{17} cm^{-2} , Braun & Thilker (2004) detected very faint HI emission in a long plume extending from M31 in the general direction of M33. Subsequent observations with the GBT at higher angular resolution showed that most of the emission was concentrated into discrete clouds (Wolfe et al., 2013, 2016). Assuming that these clouds are at a distance of 800 kpc, between M31 and M33, they have $M_{\text{HI}} = 0.4 - 3.3 \times 10^5 M_{\odot}$, sizes of a few kpc, and are not associated with any stars or stellar stream. Figure 8 shows the clouds colored by their velocities. The field lies ~ 100 kpc from M31. There are substantial differences in the velocities from cloud to cloud, $> 100 \text{ km s}^{-1}$, indicating that these are discrete objects and not simply the brighter portions of a single extended sheet. Velocity gradients across each cloud, in contrast, are only $\approx 10 \text{ km s}^{-1}$. The dynamical mass of the clouds, i.e., the mass needed for them to be self-gravitating, is typically 10^3 times more than the observed mass in HI. There are indications in the data that more clouds like these exist adjacent to the area covered by the GBT observations.

Fig. 4 shows the relationship between the M31-M33 clouds and the galaxies M31 and M33, together with their systems of HVCs. It is apparent that the M31-M33 clouds lack the large velocity spread of the HVCs, and that their kinematics has more in common with the systemic velocities of the galaxies than with their HVCs. There is no apparent connection between these clouds and the M31 system of satellite galaxies (Wolfe et al., 2016).

The M31-M33 clouds appear to be a new population in the Local Group with no known analogs. Beyond the work of Braun & Thilker (2004) and the data shown in Fig. 8, no other areas in the Local Group have been surveyed to the sensitivity necessary to detect HI emission at these faint levels. There is some indication that similar objects may exist to the north of M31 (Wolfe et al., 2016) but current data are inconclusive. Braun & Thilker (2004) initially proposed that this HI condensed

from an intergalactic filament and there are models where it arises as the result of an interaction between M31 and M33 (Bekki, 2008; Lewis et al., 2013). The later suggestion, while attractive, now seems unlikely given the past history of the Local Group (Shaya & Tully, 2013). We note that the M31-M33 clouds, like IC 10, reside well within the CGM of M31. It is estimated that the CGM has a total column density $N_{\text{H}} \approx 10^{18} \text{ cm}^{-2}$ at the location of Fig. 8 (Lehner et al., 2015). The average N_{HI} of the clouds over the entire field is only $9 \times 10^{16} \text{ cm}^{-2}$, so even if the ionization fraction of the CGM is $> 90\%$, there would still be enough neutral material to account for the clouds (Wolfe et al., 2016).

6 Starless HI Near and Far

This survey of HI in the Local Group has ranged from the disk-halo clouds, which are certainly confined to the stellar disks, through the high velocity clouds, which seem preferentially located around the disks of galaxies, to material that is not incorporated into galaxies: the Magellanic Stream and Leading Arm, the HI streams intersecting IC 10, and finally the M31-M33 clouds. The first two, at least, are associated with stellar systems, while the M31-M33 clouds are not. Their properties are summarized in Table 1. How common are objects like this in other galaxies and other groups?

The disk-halo clouds and most HVCs would be blended together in current HI observations of galaxies outside the Local Group, but similar material appears to be present in many other galaxies (see section 2). In very sensitive HI observations many, if not most spiral galaxies show HI streams or features extending from the disk. This suggests that we are witnessing interaction, even though in many cases an accreting stellar companion cannot be identified (Sancisi et al., 2008). True starless HI clouds not associated with a galaxy seem rare, existing perhaps at the level of 2% of the HI objects detected in deep surveys, and even so, many of these seem to be located near large galaxies or be associated with tidal debris (Kovač et al., 2009; Haynes et al., 2011). Some of the most interesting objects, like the M31-M33 clouds and the plumes of IC 10, could be detected only out to a few Mpc from the Milky Way with current instrumentation.

The amount of HI in starless gas in Local Group galaxies is rather modest compared to the enormous structures produced by galaxy interactions in other groups. The classic example is the M81 group (Yun et al., 1994; Chynoweth et al., 2008), but evidence for interactions like this in other galaxy groups abounds. The data are too numerous to summarize here, but as merely one example, recent observations (Leisman et al., 2016) have detected extended HI features 600 kpc in length without stellar counterparts around the NGC 3590 and NGC 3227 groups (Fig. 9).

If our Local Group is any example, the best place to detect starless neutral gas clouds is relatively close to galaxies. As deep HI surveys of the Local Group cover more area, we will obtain better insight into the origin of starless gas, and determine if it is always located near galaxies, or is more widespread.

Table 1 Inventory of Starless HI “Clouds” in the Local Group

Object	$M_{\text{HI}} (M_{\odot})$	Size (kpc)	Reference	Notes
Disk-halo clouds	7×10^2	0.06	Ford et al. (2010)	
Individual HVCs	$\sim 10^6$	2-15	Putman et al. (2012)	
All HVCs in MW, M31 or M33	$2 - 5 \times 10^7$		Westmeier et al. (2008); Putman et al. (2012); Keenan et al. (2016)	
HI stripped from MW dwarfs	3×10^7		Spekkens et al. (2014)	
IC 10 northern stream	6×10^5	7	Nidever et al. (2013); Ashley et al. (2014)	
IC 10 southern stream	$\sim 10^7$	7	Nidever et al. (2013); Ashley et al. (2014)	
Magellanic Stream	3×10^8	~ 100	Brüns et al. (2005); a Nidever et al. (2010)	
Leading Arm	3×10^7	~ 60	Putman et al. (2003)	a
M31-M33 clouds	$\sim 10^5$	2	Wolfe et al. (2016)	b
M31-M33 clouds all	$> 1.6 \times 10^6$		Wolfe et al. (2016)	b

a. Assumed distance 55 kpc. b. Assumed distance 800 kpc.

References

- Adams, E. A. K., Giovanelli, R., & Haynes, M. P. 2013, *ApJ*, 768, 77
Anderson, M. E., & Bregman, J. N. 2011, *ApJ*, 737, 22
Ashley, T., Elmegreen, B. G., Johnson, M., et al. 2014, *AJ*, 148, 130
Bekki, K. 2008, *MNRAS*, 390, L24
Blitz, L., & Robishaw, T. 2000, *ApJ*, 541, 675
Blitz, L., Spergel, D. N., Teuben, P. J., Hartmann, D., & Burton, W. B. 1999, *ApJ*, 514, 818
Braun, R., & Thilker, D. A. 2004, *A&A*, 417, 421
Braun, R., & Burton, W. B. 1999, *A&A*, 341, 437
Bregman, J. N. 1980, *ApJ*, 236, 577
Brüns, C., Kerp, J., Kalberla, P. M. W., & Mebold, U. 2000, *A&A*, 357, 120
Brüns, C., Kerp, J., Staveley-Smith, L., et al. 2005, *A&A*, 432, 45
Carlin, J. L., Beaton, R. L., Martínez-Delgado, D., & Gabany, R. J. 2016, *Astrophysics and Space Science Library*, 420, 219
Chynoweth, K. M., Langston, G. I., Yun, M. S., et al. 2008, *AJ*, 135, 1983
Dickey, J. M., & Lockman, F. J. 1990, *ARA&A*, 28, 215
D’Onghia, E., & Fox, A. J. 2016, *ARA&A*, 54, 363
Ford, H. A., Lockman, F. J., & McClure-Griffiths, N. M. 2010, *ApJ*, 722, 367
Fox, A. J., Wakker, B. P., Barger, K. A., et al. 2014, *ApJ*, 787, 147
Fox, A. J., Lehner, N., Lockman, F. J., et al. 2016, *ApJ*, 816, L11
Fraternali, F., van Moorsel, G., Sancisi, R., & Oosterloo, T. 2002, *AJ*, 123, 3124
Gerbrandt, S. A. N., McConnachie, A. W., & Irwin, M. 2015, *MNRAS*, 454, 1000
Grcevich, J., & Putman, M. E. 2009, *ApJ*, 696, 385
Grossi, M., Giovanardi, C., Corbelli, E., et al. 2008, *A&A*, 487, 161
Haynes, M. P., Giovanelli, R., Martin, A. M., et al. 2011, *AJ*, 142, 170
Heald, G., Józsa, G., Serra, P., et al. 2011, *A&A*, 526, A118
Heiles, C., 1979, *ApJ*, 229, 533
Hill, A. S., Haffner, L. M., & Reynolds, R. J. 2009, *ApJ*, 703, 1832

- Hill, A. S., Mao, S. A., Benjamin, R. A., Lockman, F. J., & McClure-Griffiths, N. M. 2013, *ApJ*, 777, 55
- Hodges-Kluck, E. J., Miller, M. J., & Bregman, J. N. 2016, *ApJ*, 822, 21
- Hopp, U., Schulte-Ladbeck, R. E., & Kerp, J. 2007, *MNRAS*, 374, 1164
- Hubble, E. 1958, *The Realm of the Nebulae*, Dover Publications, Inc.
- Kaltcheva, N. T., Golev, V. K., & Moran, K. 2014, *A&A*, 562, A69
- Kacprzak, G. G., Cooke, J., Churchill, C. W., Ryan-Weber, E. V., & Nielsen, N. M. 2013, *ApJ*, 777, L11
- Keenan, O. C., Davies, J. I., Taylor, R., & Minchin, R. F. 2016, *MNRAS* 456, 951
- Kovač, K., Oosterloo, T. A., & van der Hulst, J. M. 2009, *MNRAS*, 400, 743
- Lehner, N., Howk, J. C., & Wakker, B. P. 2015, *ApJ*, 804, 79
- Lehner, N., & Howk, J. C. 2011, *Science*, 334, 955
- Leisman, L., Haynes, M. P., Giovanelli, R., et al. 2016, *MNRAS*, in press (arXiv:1608.08986)
- Lewis, G. F., Braun, R., McConnachie, A. W., et al. 2013, *ApJ*, 763, 4
- Lockman, F. J. 1984, *ApJ*, 283, 90
- Lockman, F. J. 2002, *ApJ*, 580, L47
- Lockman, F. J. 2003, *ApJ*, 591, L33
- Lockman, F. J., Benjamin, R. A., Heroux, A. J., & Langston, G. I. 2008, *ApJ*, 679, L21
- Marasco, A., Fraternali, F., & Binney, J. J. 2012, *MNRAS*, 419, 1107
- Marasco, A., & Fraternali, F. 2017, *MNRAS*, 464, L100
- McClure-Griffiths, N. M., Dickey, J. M., Gaensler, B. M., & Green, A. J. 2002, *ApJ*, 578, 176
- McConnachie, A. W. 2012, *AJ*, 144, 4
- Miller, E. D., Bregman, J. N., & Wakker, B. P. 2009, *ApJ*, 692, 470
- Muller, C. A., Oort, J. H., & Raimond, E. 1963, *Acad. Sci. Paris Comptes Rendus*, 257, 1661
- Nichols, M., & Bland-Hawthorn, J. 2009, *ApJ*, 707, 1642
- Nichols, M., Mirabel, N., Agertz, O., Lockman, F. J., & Bland-Hawthorn, J. 2014, *MNRAS*, 442, 2883
- Nidever, D. L., Majewski, S. R., Burton, W. B., & Nigra, L. 2010, *ApJ*, 723, 1618
- Nidever, D. L., Ashley, T., Slater, C. T., et al. 2013, *ApJ*, 779, L15
- Oosterloo, T., Fraternali, F., & Sancisi, R. 2007, *AJ*, 134, 1019
- Pidopryhora, Y., Lockman, F. J., & Shields, J. C. 2007, *ApJ*, 656, 928
- Pidopryhora, Y., Lockman, F. J., Dickey, J. M., & Rupen, M. P. 2015, *ApJS*, 219, 16
- Pisano, D. J., Barnes, D. G., Gibson, B. K., et al. 2007, *ApJ*, 662, 959
- Pisano, D. J., Barnes, D. G., Staveley-Smith, L., et al. 2011, *ApJS*, 197, 28
- Putman, M. E., Staveley-Smith, L., Freeman, K. C., Gibson, B. K., & Barnes, D. G. 2003, *ApJ*, 586, 170
- Putman, M. E., Peek, J. E. G., Muratov, A., et al. 2009, *ApJ*, 703, 1486
- Putman, M. E., Peek, J. E. G., & Joung, M. R. 2012, *ARA&A*, 50, 491
- Rhode, K. L., Salzer, J. J., Haurberg, N. C., et al. 2013, *AJ*, 145, 149
- Sancisi, R., Fraternali, F., Oosterloo, T., & van der Hulst, T. 2008, *Astron. Astrophys. Rev.*, 15, 189
- Shapiro, P. R., & Field, G. B. 1976, *ApJ*, 205, 762
- Shaya, E. J., & Tully, R. B. 2013, *MNRAS*, 436, 2096
- Shull, J. M., Jones, J. R., Danforth, C. W., & Collins, J. A. 2009, *ApJ*, 699, 754
- Shull, J. M., Stevans, M., Danforth, C., et al. *ApJ*, 739, 105 (2011)
- Shostak, G. S., & Skillman, E. D. 1989, *A&A*, 214, 33
- Smith, G. P. 1963, *BAAN*, 17, 203
- Spekkens, K., Urbancic, N., Mason, B. S., Willman, B., & Aguirre, J. E. 2014, *ApJ*, 795, L5
- Stark, D. V., Baker, A. D., & Kannappan, S. J. 2015, *MNRAS*, 446, 1855
- Thilker, D. A., Braun, R., Waltherbos, R. A. M., et al. 2004, *ApJ*, 601, L39
- Tomisaka, K., & Ikeuchi, S. 1986, *PASJ*, 38, 697
- Wakker, B. P. 2004, in *High Velocity Clouds*, ed. H. van Woerden, B. P. Wakker, U. J. Schwarz, & K. S. de Boer (Dordrecht: Kluwer), 25
- Wakker, B. P., York, D. G., Wilhelm, R., et al. 2008, *ApJ*, 672, 298
- Wakker, B. P., & Savage, B. D. 2009, *ApJS*, 182, 378

- Westmeier, T., Brüns, C., & Kerp, J. 2008, MNRAS, 390, 1691
Wolfe, S. A., Pisano, D. J., Lockman, F. J., et al. 2013, Nature, 497, 224
Wolfe, S. A., Lockman, F. J., & Pisano, D. J. 2016, ApJ, 816, 81
Yun, M. S., Ho, P. T. P., & Lo, K. Y. 1994, Nature, 372, 530
Zschaechner, L. K., Rand, R. J., & Walterbos, R. 2015, ApJ, 799, 61

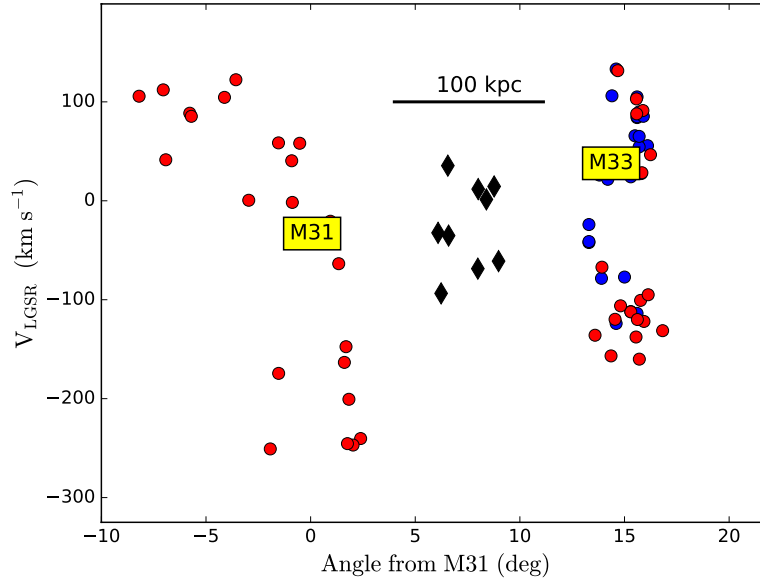


Fig. 4 The HVC systems of M31 and M33 (red circles), where the velocity with respect to the Local Group Standard of rest, V_{LGSR} , is plotted against the angular distance from M31 in the direction of M33. To the samples of M31 and M33 HVCs (Westmeier et al., 2008; Keenan et al., 2016) are added clouds that may be in the halo of M33 (blue circles) (Grossi et al., 2008; Putman et al., 2009). It can be difficult to distinguish between the two groups, which may actually blend together. The systemic velocities of M31 and M33 are indicated. Diamonds mark the M31-M33 clouds discussed in section 5.2. They have velocities more in common with the systemic velocity of M31 and M33 than of their system of HVCs. There are no stars in any of these clouds.

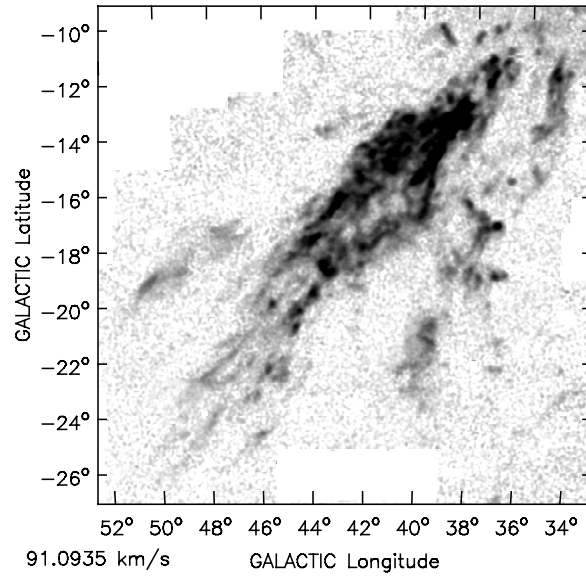


Fig. 5 Channel map of the Smith Cloud from new GBT data. All the emission in this figure is associated with the Cloud, which has other components extending down to latitude -40° . The part of the Cloud displayed in this image is about 4 kpc in length. The Galactic plane lies above this figure, and the Cloud is moving toward it at an angle.

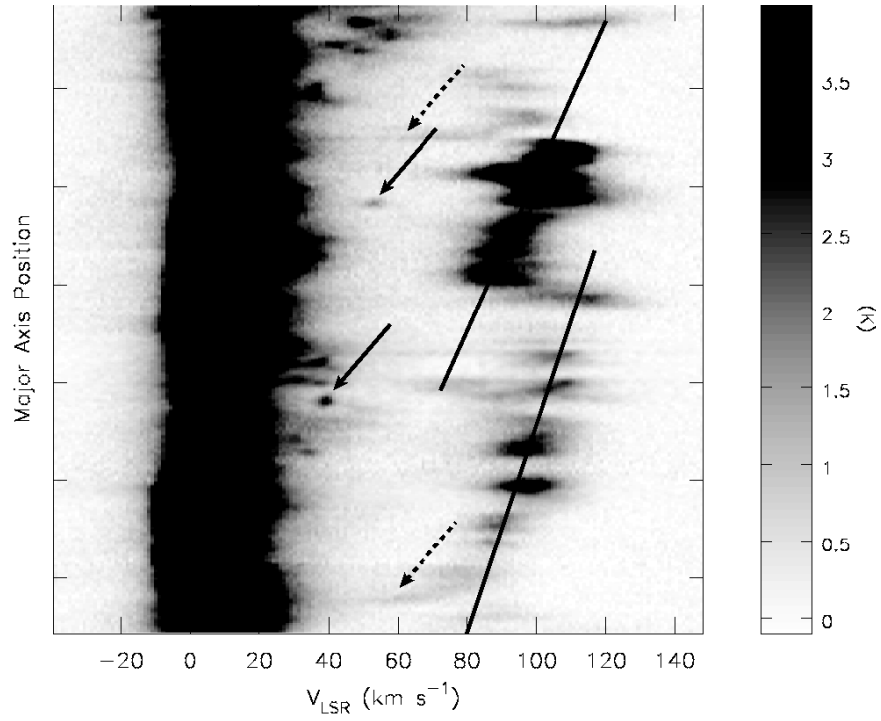


Fig. 6 A velocity-position plot down the major axis of the Smith Cloud from Lockman et al. (2008). Arrows mark lumps or streams of HI that have been decelerated by interaction with the Milky Way halo. Besides a general stripping and deceleration of the cloud edges (HI indicated by dashed arrows), it appears that the Cloud is encountering dense lumps in the Milky Way disk-halo interface that remove chunks of the Cloud (noted with solid arrows). Some of these correspond in detail to voids in the body of the Smith Cloud.

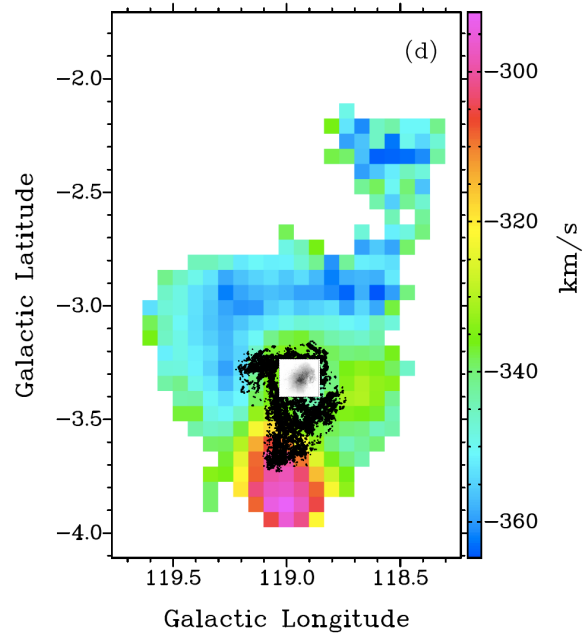


Fig. 7 Composite image of the stars and HI of IC 10 adapted from Ashley et al. (2014). Colors show the HI velocity field, highlighting the plume to the north. Black shows N_{HI} in the inner regions from a high-resolution map, showing the gas extension to the south. The insert shows the stars of IC 10 in the optical V-band.

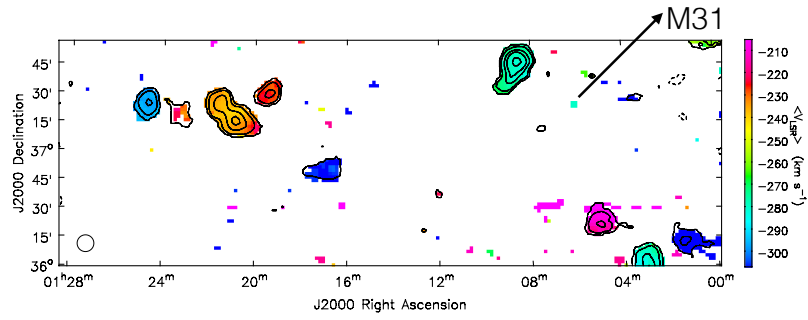


Fig. 8 Discrete HI clouds found in a region about 100 kpc away from M31 in the direction of M33 (adapted from Wolfe et al., 2016). These are also displayed as the diamonds in Fig. 4. Contours mark N_{HI} in units of $5 \times 10^{17} \text{ cm}^{-2}$, scaled by -1 (dashed), 1, 2, 4, 6, 10. The typical cloud has $M_{\text{HI}} = 10^5 M_{\odot}$. M31 lies to the upper right in the direction of the arrow; M33 to the lower left.

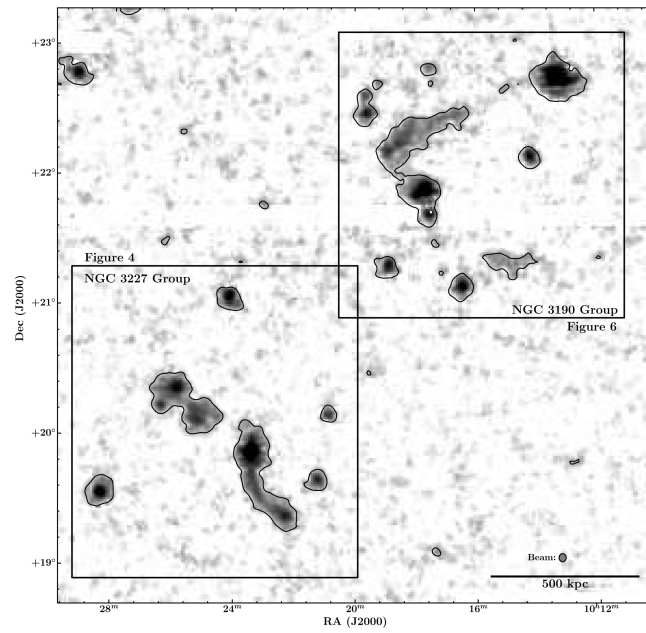


Fig. 9 Map of the HI around the NGC 3190 and NGC 3227 groups, showing extended tails and intragroup gas probably resulting from interactions between galaxies (from Leisman et al., 2016).